An analytical wave solution for the vibrational response and energy of an axially translating string in any propagation cycle

Yuteng He[a], Enwei Chen [a,*], Weidong Zhu[b], Neil.S. Ferguson[c],

Yuanfeng Wu[a], Yimin Lu[a]

[a]*School of Mechanical Engineering, Hefei University of Technology, Hefei, 230009, China*

[b]*Department of Mechanical Engineering, University of Maryland, Baltimore County, Baltimore, MD 21250, USA*

[c]*Institute of Sound and Vibration Research, University of Southampton, Southampton SO171BJ, England, UK*

**Abstract**

An axially traveling string system, which is a kind of traveling material, attracts considerable attention owing to its broad applications. In this paper, an analytical wave solution for the vibration and energy of an axially traveling string with fixed and viscous damper (dashpot) boundaries in any propagation cycle is considered. Firstly, a novel recursive and simplified technique is proposed to expand the analytical solution for a traveling string to any propagation cycle, which was limited to only one propagation cycle due to complexity in previous work. As a kind of analytical solution, the traveling wave method has more accuracy and efficiency compared to numerical methods. Secondly, different from the previous result, the modified Hamilton's principle is applied to the derivation of the dashpot boundary condition for the mass changing of the traveling string. Following the pipeline hydrodynamics theory, the energy gradient for the '*control volume*' and the '*system*' of traveling string are accurately obtained, respectively. Thirdly, from the point of view of vibration suppression, the optimal damping at the right end of the string is defined and the optimal damping value is derived, which is of considerable practical interest in vibration suppression at boundaries for axially traveling materials.

**Keywords:** analytical; traveling string; energy; vibration suppression

## 1. Introduction

The model of the traveling material is widely applied in many mechanical engineering systems, such as slurry wire saw [1], zinc galvanization, textile and composite fibers, pipes conveying fluid, etc [2, 3]. With negligible bending stiffness of the traveling material [2], such as threads in the textile processes and narrow belts, the system can be simplified as a model of an axially traveling string. In these systems, the mechanical vibration of the transported materials is a significant problem that has an adverse effect on the overall performance. Hence, appropriate vibration control can reduce noise, make a good performance of the structures, and even avoid security issues. To determine the parameters for the design of vibration control, vibration behaviors are usually studied by solving the governing equation of motion. The earlier investigations have been reviewed by Hong and Pham [4]. Recent developments of the traveling wave solution (or d'Alembert's solution) of an axially traveling string, which is the focus of this paper, can be achieved by Gaiko and Van Horssen [5] and Chen et al.[6-9].

As a classical solution, the Fourier series method has been used for stationary continuous systems such as beams [10] and shells [11], as well as for axially traveling string with fixed boundaries [12-14], yet it has not been applied to nonclassical boundaries with mass, damping or spring, due to the difficulty of satisfying the complex boundary conditions. In addition, Fourier series method is approximate since the limited number of terms to be expanded. The method of d'Alembert is another classical solution, which is suitable for an infinite non-traveling string. The method of d'Alembert was applied to a string without boundaries in earlier investigations. Swope and Ames [15] extended it to an infinite traveling string. From the time domain, the d'Alembert solution gives an exact solution for the translating motion of the string. Nevertheless, when boundaries are considered, the situation becomes more complex for the reflection and transmission of traveling waves.

Recently, there has been some headway for the application of traveling wave solution on a finite or traveling medium. The response of a finite rod with two damped boundaries is obtained by Sirota and Halevi [16]. Gaiko and van Horssen [5] studied the reflection phenomena of a semi-infinite traveling string with a non-classical boundary. And this investigation exerts a profound effect on our studies. Chen et al.[6-9, 17] extended the d'Alembert's solution to a finite traveling string with various boundary conditions. Due to multiple reflections, the reflected wave superposition method was proposed for a traveling string with two boundaries. Compared to some numerical solutions (e.g., the Galerkin method, the finite element method, the Runge-Kutta method, etc.) and approximate solutions (e.g., the perturbation technique, the Fourier series method, etc.) [2], the proposed reflected wave superposition method is analytical, which has high accuracy, can strictly satisfy the classical and nonclassical boundary conditions and does not need the frequency spectrum and eigenfunctions [5].

However, the analytical solutions are only suitable for the first propagation cycle $T$. Based on prior investigations about the reflected wave superposition method, some extensions and modifications will be presented in this paper.

As a mass variable system with the axial motion, a traveling string with boundaries is treated as a special kind of fluid-conveying [3, 18] because they have a familiar governing equation. It is essential to add or modify some theories and methods according to fluid mechanics, which is a relatively mature theory. Firstly, as usually formulated, traditional Hamilton's principle isn't suitable for an open system of changing mass. Modified Hamilton's principle has been derived and proved by [19, 20]. For example, Kim [21] used the modified Hamilton's principle when studied the boundary control of an axially traveling string. However, in recent decades, some investigations ignore this modification. Secondly, it is essential to clarify whether the gradient of system or that of control volume is analyzed when analyzing the change of energetics. Initially, Renshaw et al. [22] analyzed the energetics of traveling string from Lagrangian viewpoint and Eulerian viewpoint. Drawing on concepts from fluid mechanics, Zhu [23] distinguished energy gradient of translating media from system and control volume viewpoints, which correspond to Lagrangian and Eulerian viewpoints respectively. It is instructive to consider the energy change of a traveling string from these two different perspectives for this paper.

This paper pays attention to the response and energy of an axially traveling string with mixed boundaries. Analytical solutions of transverse displacement and energy are obtained by using a traveling wave method. Firstly, the solution for an axially traveling string with fixed_dashpot boundaries is extended to any propagation cycle by a novel recursive and simplified technique. Secondly, the change of energy for a traveling string is considered from two different viewpoints. Based on fluid mechanics, *control volume* characterizes the stability, and *system* links energy with instantaneous work [23]. Thirdly, with a different method, the result of the optimal damping in this paper is the same as [24]. And the optimal damping is obtained, proved and explained in time domain. Obtaining an optimal damping at the dashpot boundary is very valuable for the design of active or passive control of dampers involving axially moving devices, such as wire saw, textile equipment, conveyor belt, etc.

This paper is organized as follows. Section 2 shows the governing equation of motion and the boundary value problem. In section 3, the displacement response in the form of traveling waves is derived by the application of the traveling wave method. In section 4, the energy and its gradient of the traveling waves at any time interval are derived. In section 5, results of the simulations are shown for the response and energy. Finally, section 6 provides the conclusions.

## 2. Equations of motion and boundary value problem

This paper focuses on the analytical method for the vibration of traveling string in any propagation cycle. It is worth to note that this method is applicable to general boundary conditions, including classical and nonclassical ones. For simplicity, a traveling string with the left end fixed and the right end supported by a viscous damper presented in Fig.1 is adopted, which are subsequently named fixed_dashpot boundaries in this paper. For the actual engineering case of traveling string, more complex boundaries, such as mass-dashpot-spring boundaries, are required, yet the calculation principle and process are consistent with the method of fixed_dashpot boundaries. For general impedance boundary cases of traveling string models, such as mass-dashpot-spring boundary, the main recursive formulas for the waves reflected from this boundary are given in Appendix B.

In Fig.1, $l_0$ is the length of the string between the boundaries; $x$ is a fixed spatial coordinate system, which represents the axial position of a point in the string from the fixed end; $u(x, t)$ represents the transverse displacement of the axially traveling string at the coordinate $x$ and time $t$; $v$ is the constant translational speed of the string and $\eta$ is the viscous damping coefficient at the right boundary. In this paper, the vibrational response and energy of the traveling string system in any propagation cycle shown in Fig. 1 are investigated.

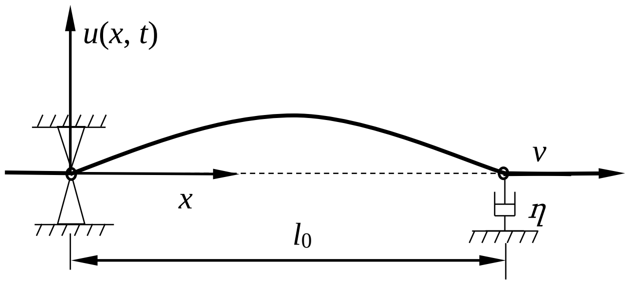


**Fig. 1** Traveling string with fixed_dashpot boundaries.

The governing equation of motion can be obtained [5, 7, 24]

$$u_{tt} + 2vu_{xt} + \left(v^2 - c^2\right)u_{xx} = 0 \tag{1}$$

and the boundary conditions are given as follows.

$$\begin{cases} u\left(0,t\right) = 0 \\ \eta u_t\left(l_0,t\right) = -Pu_x\left(l_0,t\right) \end{cases} \tag{2}$$

where the subscripts denote the partial derivatives of $u(x, t)$ with respect to the corresponding variable. The parameter of $c$ is the free wave propagation speed given by $c = \sqrt{P/\rho}$, where $P$ is the uniform tension in the string and $\rho$ is the uniform string mass per unit length. For the reliability of the predictions from linear theory [25], the case of super-critical speed is not considered. Hence, the string translational speed $v$ is assumed to be less than the free wave propagation speed $c$, i.e. $|v| < c$. It should be noted that the damping boundary conditions given in Eq. (2) are different from the one given in [5] shown as follows.

$$(\eta - \rho v)u_t\left(l_0,t\right) = (\rho v^2 - P)u_x\left(l_0,t\right) \tag{3}$$

The main reason is that the modified Hamilton's principle, instead of the traditional one, should be used for the mass change system such as axially traveling string. For a closed system, the traditional Hamilton's principle is

$$\delta\int_{t_1}^{t_2} L\mathrm{d}t + \int_{t_1}^{t_2} \delta W\mathrm{d}t = 0 \tag{4}$$

Here, $\delta$ is a variation in a function and $\delta W$ is the virtual work done by nonconservative forces. The Lagrangian of $L$ is equal to $E_k$ - $E_p$, where $E_k$ and $E_p$ are the kinetic energy and potential energy of the system, respectively. The integration interval is between two instants of time $t_1$ and $t_2$. For an axially traveling string system, the modified Hamilton's principle [20] is

$$\delta\int_{t_1}^{t_2} L\mathrm{d}t + \int_{t_1}^{t_2} \delta W\mathrm{d}t - \int_{t_1}^{t_2} \left.(\rho v(u_t + vu_x)\delta u)\right|_0^{l_0} \mathrm{d}t = 0 \tag{5}$$

which is used for the correct derivation of the damping boundary condition Eq. (2). The complete derivation process for the damping boundary condition in Eq. (2) is given in Appendix A.

## 3. Solution

The general solution for the second-order partial differential Eq. (1) is [6, 15]

$$u(x,t) = F(x - v_r t) + G(x + v_l t) \tag{6}$$

where $F(x - v_r t)$ is the right-propagating wave with a speed of $v_r = c + v$ and $G(x + v_l t)$ is the left-propagating wave with a speed of $v_l = c - v$, related to the fixed coordinate system. The initial transverse displacement and velocity conditions for the string vibration are given as follows.

$$\begin{cases} u(x,0) = \phi(x) \\ u_t(x,0) = \psi(x) \end{cases}, 0 \le x \le l_0 \tag{7}$$

where $\Phi(x) \in C^2([0,l_0]; \mathrm{R})$ and $\psi(x) \in C^1([0,l_0]; \mathrm{R})$. Substituting Eq. (6) into Eq. (7), one obtains the expressions for $F(x)$ and $G(x)$ as follows.

$$\begin{cases} F(x) = \dfrac{v_l}{v_r + v_l}\phi(x) - \dfrac{1}{v_r + v_l}\displaystyle\int_{x_1}^{x} \psi(\xi)\,\mathrm{d}\xi \\ G(x) = \dfrac{v_r}{v_r + v_l}\phi(x) + \dfrac{1}{v_r + v_l}\displaystyle\int_{x_1}^{x} \psi(\xi)\,\mathrm{d}\xi \end{cases} \tag{8}$$

where $x_1$ is an arbitrary constant and, in this paper, $x_1 = 0$ for convenience.

### 3.1 The expressions of traveling waves for the first cycle

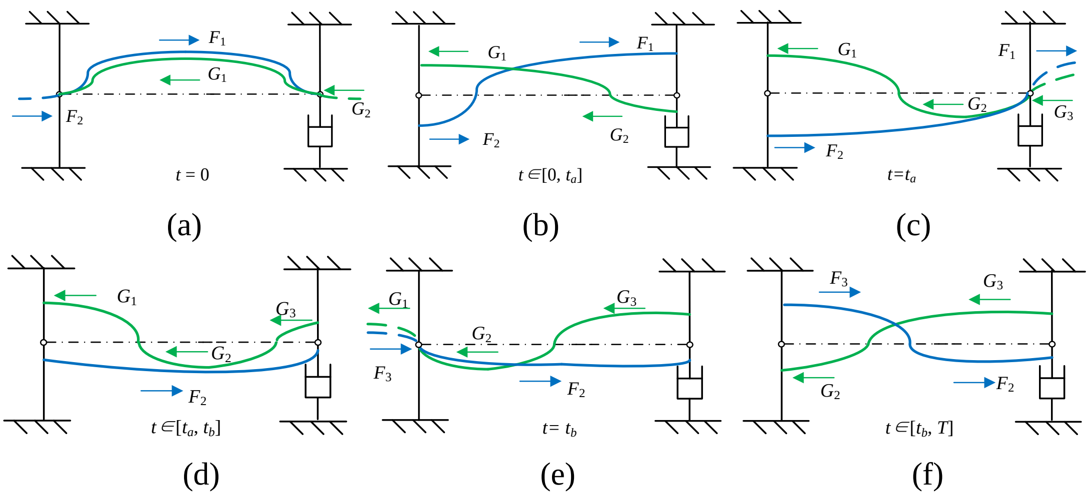


**Fig. 2** The propagating waves in a traveling string during three time intervals in one cycle. (a) is for $t = 0$, (b) is for $t \in [0, t_a]$, (c) is for $t = t_a$, (d) is for $t \in [t_a, t_b]$, (e) is for $t = t_b$ and (f) is for $t \in [t_b, T]$. The waves of $F_2$, $G_2$, $F_3$ and $G_3$ are the reflections of waves $G_1$, $F_1$, $G_2$ and $F_2$, respectively.

Fig. 2 shows the reflection process of the left-propagating waves $G_i$ and the right-propagating waves $F_i$ ($i$ = 1, 2, 3) in one cycle. The cycle $T$ for a propagating wave in a traveling string, which is defined in the introduction section, is given by [3]

$$T = \frac{l_0}{v_r} + \frac{l_0}{v_l} = \frac{2cl_0}{c^2 - v^2} \tag{9}$$

and the definitions as well as the detailed expressions for $t_a$ and $t_b$ are shown in the reflected wave superposition method given in [22]

$$\begin{cases} t_a = l_0 / v_r \\ t_b = l_0 / v_l \end{cases} \tag{10}$$

The traveling waves are divided into several segments artificially for reflection. $G_1$ and $F_1$ are initial traveling waves. $G_3$ and $F_3$ are final traveling waves. $G_{i+1}$ and $F_{i+1}$ are reflected by incident waves $F_i$ and $G_i$ respectively.

By substituting Eq. (6) into Eq. (2), the boundary reflection relationships at the left and right hand boundaries respectively are

$$F(-v_r t) = -G(v_l t) \tag{11}$$

$$G'(l_0 + v_l t) = \beta F'(l_0 - v_r t) \tag{12}$$

where $\beta = \dfrac{\eta v_r - P}{\eta v_l + P}$. Combing Fig. 2, Eq. (11) states that the left-propagating waves $G_i$ produces the right-propagating waves $F_{i+1}$ when $G_i$ reaches the upstream ($x$ = 0). Similarly, Eq. (12) states that $F_i$ produces $G_{i+1}$ when $F_i$ reaches the downstream ($x$ = $l_0$). Eq. (11) and Eq. (12) become

$$F(r) = -G(-\frac{v_l}{v_r} r) \tag{13}$$

and

$$G'(s) = \beta F'(\frac{2cl_0}{v_l} - \frac{v_r}{v_l} s) \tag{14}$$

respectively, by setting $r = -v_r t$ and $s = l_0 + v_l t$.

Since the time periods of $G_2$ and $G_3$ are [0, $t_a$]and [$t_a$, $T$] respectively, the integral intervals corresponding to Eq. (14) are [$l_0$, $x$] and [$l_0+v_l t_a$, $x$], respectively. After integrating and simplifying Eq. (14) in the above integral intervals, $G_2$ and $G_3$ can be obtained

$$G_2(x) = G_2(l_0) + \beta \frac{v_l}{v_r} F_1(l_0) - \beta \frac{v_l}{v_r} F_1\left(\frac{2c}{v_l} l_0 - \frac{v_r}{v_l} x\right) \tag{15}$$

$$G_3(x) = G_3(l_0 + v_l t_a) + \beta \frac{v_l}{v_r} F_2(l_0 - v_r t_a) - \beta \frac{v_l}{v_r} F_2\left(\frac{2c}{v_l} l_0 - \frac{v_r}{v_l} x\right) \tag{16}$$

The waves $F_2$ and $F_3$ are obtained by using Eq. (13) as follows.

$$F_2(x) = -G_1(-\frac{v_l}{v_r} x) \tag{17}$$

$$F_3(x) = -G_2(-\frac{v_l}{v_r} x) \tag{18}$$

The corresponding traveling wave expressions are

$$G_2(x + v_l t) = G_2(l_0) + \beta \frac{v_l}{v_r} F_1(l_0) - \beta \frac{v_l}{v_r} F_1(\frac{2cl_0}{v_l} - \frac{v_r}{v_l}(x + v_l t)) \tag{19}$$

$$F_2(x - v_r t) = -G_1(-\frac{v_l}{v_r}(x - v_r t)) \tag{20}$$

$$G_3\left(x+v_l t\right)=G_3\left(l_0+v_l t_a\right)+\beta\frac{v_l}{v_r}F_2\left(l_0-v_r t_a\right)-\beta\frac{v_l}{v_r}F_2(\frac{2cl_0}{v_l}-\frac{v_r}{v_l}(x+v_l t)) \tag{21}$$

$$F_3\left(x-v_r t\right)=-G_2(-\frac{v_l}{v_r}(x-v_r t)) \tag{22}$$

where $G_2(l_0)=G_1(l_0)$ and $G_3(l_0+v_l t_a)= G_2(l_0+v_l t_a)$ due to the continuity condition. Eqs. (19) to (22) are the boundary reflection relationships for the fixed_dashpot boundary condition.

### 3.2 The expressions of the traveling waves for the $n^{th}$ cycle

By applying techniques similar to Section 3.1, the relationship between $F_i^n(x - v_r t)$ and $G_i^n(x + v_l t)$ ($i$ = 1, 2, 3) similar to Eqs. (19) to (22) can be obtained where $F_i^n(x - v_r t)$ and $G_i^n(x + v_l t)$ are the right-propagating wave and the left-propagating wave in the $n^{th}$ cycle, respectively

$$G_2^n\left(x\right)=G_2^n\left(l_0+v_l(n-1)T\right)+\beta\frac{v_l}{v_r}F_1^n\left(l_0-v_r(n-1)T\right)-\beta\frac{v_l}{v_r}F_1^n(\frac{2c}{v_l}l_0-\frac{v_r}{v_l}x) \tag{23}$$

$$G_3^n\left(x\right)=G_3^n\left(l_0+v_l((n-1)T+t_a)\right)+\beta\frac{v_l}{v_r}F_2^n\left(l_0-v_r((n-1)T+t_a)\right)-\beta\frac{v_l}{v_r}F_2^n(\frac{2c}{v_l}l_0-\frac{v_r}{v_l}x) \tag{24}$$

$$F_2^n(x)=-G_1^n(-\frac{v_l}{v_r}x) \tag{25}$$

$$F_3^n(x)=-G_2^n(-\frac{v_l}{v_r}x) \tag{26}$$

By substituting Eq. (25) into Eq. (24) and substituting Eq. (23) into Eq. (26), the relationships between the initial waves ($G_1^n$ and $F_1^n$) and the end waves ($G_3^n$ and $F_3^n$) in the $n^{th}$ cycle can be obtained as follows.

$$G_3^n\left(x+v_l t\right)=G_3^n\left(l_0+v_l((n-1)T+t_a)\right)+\beta\frac{v_l}{v_r}F_2^n\left(l_0-v_r((n-1)T+t_a)\right)+\beta\frac{v_l}{v_r}G_1^n(-\frac{2cl_0}{v_r}+(x+v_l t)) \tag{27}$$

$$F_3^n\left(x-v_r t\right)=-G_2^n\left(l_0+v_l(n-1)T\right)-\beta\frac{v_l}{v_r}F_1^n\left(l_0-v_r(n-1)T\right)+\beta\frac{v_l}{v_r}F_1^n(\frac{2cl_0}{v_l}+(x-v_r t)) \tag{28}$$

It should be noted that the initial waves ($F_1^{n+1}$ or $G_1^{n+1}$) in the $(n + 1)^{th}$ cycle are exactly the end waves ($F_3^n$ or $G_3^n$) in the $n^{th}$ cycle due to periodicity. Therefore, the relationship between the right-propagating waves (or the left-propagating wave) in two adjacent cycles can be obtained as follows.

$$F_3^n(x-nv_r T)=F_1^{n+1}(x-nv_r T) \quad or \quad F_3^n=F_1^{n+1} \tag{29}$$

$$G_3^n(x+nv_l T)=G_1^{n+1}(x+nv_l T) \quad or \quad G_3^n=G_1^{n+1} \tag{30}$$

Finally, according to Eqs. (27) to (30), one can obtain the relationships between the initial waves in the $n^{th}$ cycle and the initial waves in the first cycle as follows.

$$\begin{aligned}F_1^n(x-v_r t)=&-\sum_{j=1}^{n-1}(\beta\frac{v_l}{v_r})^{n-j-1}G_2^j(l_0+v_l(j-1)T)-\sum_{j=1}^{n-1}(\beta\frac{v_l}{v_r})^{n-j}F_1^j(l_0-v_r(j-1)T)\\&+(\beta\frac{v_l}{v_r})^{n-1}F_1^1((n-1)\frac{2cl_0}{v_l}+x-v_r t)\end{aligned} \tag{31}$$

$$G_1^n(x+v_lt)=\sum_{j=1}^{n-1}(\beta\frac{v_l}{v_r})^{n-j-1}G_3^{\,j}(l_0+v_l(t_a+(j-1)T))+\sum_{j=1}^{n-1}(\beta\frac{v_l}{v_r})^{n-j}F_2^{\,j}(l_0-v_r(t_a+(j-1)T))$$
$$+(\beta\frac{v_l}{v_r})^{n-1}G_1^1(-(n-1)\frac{2cl_0}{v_r}+x+v_lt) \tag{32}$$

Further, the relationships between other waves of $F_2^n$, $F_3^n$, $G_2^n$ and $G_3^n$ for the $n^{th}$ cycle and the initial waves of $G_1^1$ and $F_1^1$ for the first cycle can be obtained as follows according to the boundary reflection relationships.

$$F^n{}_2\left(x-v_rt\right)=-\sum_{j=1}^{n-1}(\beta\frac{v_l}{v_r})^{n-j-1}G_3^{\,j}\left(l_0+v_l(t_a+(j-1)T)\right)-\sum_{j=1}^{n-1}(\beta\frac{v_l}{v_r})^{n-j}F_2^{\,j}\left(l_0-v_r(t_a+(j-1)T)\right)$$
$$-(\beta\frac{v_l}{v_r})^{n-1}G_1^1(-\left(n-1\right)\frac{2cl_0}{v_r}-\frac{v_l}{v_r}(x-v_rt)) \tag{33}$$

$$G^n{}_2\left(x+v_lt\right)=\sum_{j=1}^{n}(\beta\frac{v_l}{v_r})^{n-j}G_2^{\,j}\left(l_0+v_l(j-1)T\right)+\sum_{j=1}^{n}(\beta\frac{v_l}{v_r})^{n-j+1}F_1^{\,j}\left(l_0-v_r(j-1)T\right)$$
$$-(\beta\frac{v_l}{v_r})^{n}F_1^1(n\frac{2cl_0}{v_l}-\frac{v_r}{v_l}(x+v_lt)) \tag{34}$$

$$F^n{}_3\left(x-v_rt\right)=-\sum_{j=1}^{n}(\beta\frac{v_l}{v_r})^{n-j}G_2^{\,j}\left(l_0+v_l(j-1)T\right)-\sum_{j=1}^{n}(\beta\frac{v_l}{v_r})^{n-j+1}F_1^{\,j}\left(l_0-v_r(j-1)T\right)$$
$$+(\beta\frac{v_l}{v_r})^{n}F_1^1(n\frac{2cl_0}{v_l}+x-v_rt) \tag{35}$$

$$G^n{}_3\left(x+v_lt\right)=\sum_{j=1}^{n}(\beta\frac{v_l}{v_r})^{n-j}G_3^{\,j}\left(l_0+v_l(t_a+(j-1)T)\right)+\sum_{j=1}^{n}(\beta\frac{v_l}{v_r})^{n-j+1}F_2^{\,j}\left(l_0-v_r(t_a+(j-1)T)\right)$$
$$-(\beta\frac{v_l}{v_r})^{n}G_1^1(-n\frac{2cl_0}{v_r}+x+v_lt) \tag{36}$$

where

$$G_2^{\,j}(l_0+v_l(j-1)T)=G_1^{\,j}(l_0+v_l(j-1)T)$$

and

$$G_3^{\,j}(l_0+v_l(t_a+(j-1)T))=G_2^{\,j}(l_0+v_l(t_a+(j-1)T)$$

due to the continuity conditions. It should be noted that the first two terms on the right of the equal signs of Eqs. (31) to (36) are in the form of constant superposition, which means that the multi-cycle algorithm is very efficient.

## 4. Energy of traveling waves in any propagation cycle

In this section, the research object is the change of energy for an axially traveling string, which should be analyzed from two different viewpoints, i.e. the energy gradient for *control volume* and the energy gradient for *system*. Here, *control volume* means a selected region in space [26], and *system* means a quantity of matter that consists of a fixed amount of mass, which are shown in Fig. 3.

Whether to study the energy of traveling string system from the perspective of control volume or system mainly depends on whether a volume in space or a fixed amount of material is suitable for study [26]. '*Control volume*' is more suitable for the axially traveling string with two boundaries, which provides a method for what effect the response of the string has on a particular volume in space. Sometimes, one may focus on what happens to a particular part of a string as it moves through the domain. Then, the energy gradient for '*system*' becomes the main object for study.

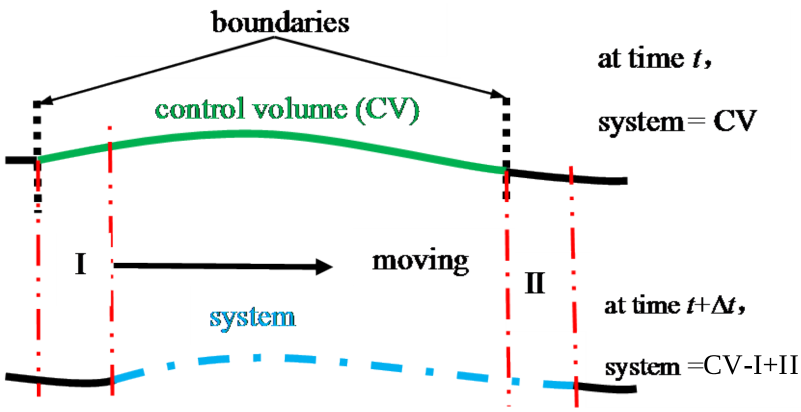


**Fig. 3** Illustration of the description of the control volume and system for a translating string at time $t$ and $t+\Delta t$

In Fig. 3, the relationships of energy for control volume $E_{\mathrm{CV}}$ and energy for system $E_{\mathrm{sys}}$ at time $t$ and $t+\Delta t$, respectively, are shown and given as follows.

$$E_{\mathrm{sys}}(t) = E_{\mathrm{CV}}(t) \tag{37}$$

$$E_{\mathrm{sys}}(t+\Delta t) = E_{\mathrm{CV}}(t+\Delta t) - E_{\mathrm{I}}(t+\Delta t) + E_{\mathrm{II}}(t+\Delta t) \tag{38}$$

By combining Eq. (37) and Eq. (38), the change of $E_{\mathrm{sys}}$ in the time interval $\Delta t$ divided by this time interval is given by

$$\frac{E_{\mathrm{sys}}(t+\Delta t) - E_{\mathrm{sys}}(t)}{\Delta t} = \frac{E_{\mathrm{CV}}(t+\Delta t) - E_{\mathrm{CV}}(t)}{\Delta t} - \frac{E_{\mathrm{I}}(t+\Delta t)}{\Delta t} + \frac{E_{\mathrm{II}}(t+\Delta t)}{\Delta t} \tag{39}$$

As $\Delta t \to 0$, using the definition of derivative yields the relationship between the gradient for $E_{\mathrm{sys}}$ and the gradient for $E_{\mathrm{cv}}$, i.e. the Reynolds transport theorem [23, 26-28].

$$\frac{\mathrm{d}E_{\mathrm{sys}}}{\mathrm{d}t} = \frac{\mathrm{d}E_{\mathrm{CV}}}{\mathrm{d}t} - v\varepsilon(0,t) + v\varepsilon(l_0,t) = \frac{\mathrm{d}E_{\mathrm{CV}}}{\mathrm{d}t} + v\varepsilon\Big|_0^{l_0} \tag{40}$$

where $\varepsilon$ is the total energy density.

The traveling wave energy is given by [9]

$$\begin{aligned} E_{\mathrm{CV}}(t) &= \int_0^{l_0}\left(\frac{1}{2}\rho v^2 + \frac{1}{2}\rho(u_t + vu_x)^2 + \frac{1}{2}Pu_x{}^2\right)\mathrm{d}x \\ &= \rho c^2 \int_0^{l_0}(F'^2 + G'^2)\,\mathrm{d}x + \frac{1}{2}\rho v^2 l_0 \end{aligned} \tag{41}$$

here

$$\begin{cases} u_t = -v_r F' + v_l G' \\ u_x = F' + G' \end{cases} \tag{42}$$

which can be obtained by Eq. (6). The energy in Eq. (41) belongs to energy for a control volume (open system) [26]. The gradient for $E_{\mathrm{CV}}(t)$ is given by

$$\begin{aligned} \frac{\mathrm{d}E_{\mathrm{CV}}}{\mathrm{d}t} &= \rho(c^2 - v^2)u_t u_x\Big|_0^{l_0} - \frac{\rho v}{2}u_t{}^2\Big|_0^{l_0} + \frac{\rho(c^2-v^2)v}{2}u_x{}^2\Big|_0^{l_0} \\ &= \rho c^2[-v_r F'^2(x - v_r t) + v_l G'^2(x + v_l t)]\Big|_0^{l_0} \end{aligned} \tag{43}$$

The total energy density $\varepsilon$ in Eq. (40) is given by

$$\varepsilon=\frac{1}{2}\rho v^2+\frac{1}{2}\rho(u_t+vu_x)^2+\frac{1}{2}Pu_x{}^2 \tag{44}$$

Substituting Eq. (42) into Eq. (44), one can obtain

$$\varepsilon=\frac{1}{2}\rho v^2+\rho c^2(F'^2+G'^2) \tag{45}$$

Substituting Eq. (45) and Eq. (43) into Eq. (40) yields the energy gradient for system

$$\begin{aligned}\frac{\mathrm{d}E_{\mathrm{sys}}}{\mathrm{d}t}&=c^2\rho(u_tu_x+vu_x{}^2)\Big|_0^{l_0}=(Pu_x)(u_t+vu_x)\Big|_0^{l_0}\\&=\rho c^2[-v_rF'^2(x-v_rt)+v_lG'^2(x+v_lt)]\Big|_0^{l_0}+[\frac{1}{2}\rho v^3+\rho c^2v(F'^2(x-v_rt)+G'^2(x+v_lt))]\Big|_0^{l_0}\end{aligned} \tag{46}$$

Eq. (46) reveals that the energy gradient for system equals the rate of work done by the transverse forces ($Pu_x$) at both boundaries on the string with transverse velocity ($u_t$+$vu_x$). Simplifying Eq. (46) yields

$$\frac{\mathrm{d}E_{\mathrm{sys}}}{\mathrm{d}t}=\rho c^2[(v-v_r)F'^2(x-v_rt)+(v+v_l)G'^2(x+v_lt)]\Big|_0^{l_0}=\rho c^3[-F'^2(x-v_rt)+G'^2(x+v_lt)]\Big|_0^{l_0} \tag{47}$$

**4.1 Derivation of the energy expressions in any propagation cycle**

The expressions for the traveling waves were obtained in section 3, the corresponding energy and its gradient are derived as follows.

Differentiating Eq. (31) yields

$$\left[F_1^n\left(x-v_rt\right)\right]'=\left(\beta\frac{v_l}{v_r}\right)^{n-1}F'^{\,1}_1\left[(n-1)\frac{2c}{v_l}l_0+x-v_rt\right] \tag{48}$$

Substituting Eq. (48) into Eq. (41) yields

$$\begin{aligned}E_{F_1^n}(t)_{x_1,x_2}&=\rho c^2\int_{x_1}^{x_2}\left[F'^{\,n}_1\left(x-v_rt\right)\right]^2\mathrm{d}x\\&=\rho c^2\int_{x_1}^{x_2}\left[\left(\beta\frac{v_l}{v_r}\right)^{n-1}F'^{\,1}_1\left[(n-1)\frac{2c}{v_l}l_0+x-v_rt\right]\right]^2\mathrm{d}x\end{aligned} \tag{49}$$

where $E_{F_1^n}(t)_{x_1,x_2}$ represents the mechanical energy of the propagating wave $F_1$ in the range of $x_1$ to $x_2$, $0 < x_1 < x_2 < l_0$. In the same way, the energy expressions for the propagating waves $F_2$, $F_3$, $G_1$, $G_2$ and $G_3$in the $n^{th}$ cycle can be written as

$$E_{F_2^n}(t)_{x_1,x_2}=\rho c^2\int_{x_1}^{x_2}\left\{\frac{v_l}{v_r}\left(\beta\frac{v_l}{v_r}\right)^{n-1}G'^{\,1}_1\left[-(n-1)\frac{2c}{v_r}l_0-\frac{v_l}{v_r}(x-v_rt)\right]\right\}^2\mathrm{d}x \tag{50}$$

$$E_{F_3^n}(t)_{x_1,x_2}=\rho c^2\int_{x_1}^{x_2}\left\{\left(\beta\frac{v_l}{v_r}\right)^{n}F'^{1}_1\left[n\frac{2c}{v_l}l_0+x-v_rt\right]\right\}^2\mathrm{d}x \tag{51}$$

$$E_{G_1^n}(t)_{x_1,x_2}=\rho c^2\int_{x_1}^{x_2}\left\{\left(\beta\frac{v_l}{v_r}\right)^{n-1}G'^{\,1}_1\left[-(n-1)\frac{2c}{v_r}l_0+x+v_lt\right]\right\}^2\mathrm{d}x \tag{52}$$

$$E_{G_2^n}\left(t\right)_{x_1,x_2}=\rho c^2\int_{x_1}^{x_2}\left\{\frac{v_r}{v_l}.\left(\beta\frac{v_l}{v_r}\right)^n F'^{1}_{1}\left[n\frac{2c}{v_l}l_0-\frac{v_r}{v_l}x-v_r t\right]\right\}^2\mathrm{d}x \tag{53}$$

$$E_{G_3^n}\left(t\right)_{x_1,x_2}=\rho c^2\int_{x_1}^{x_2}\left\{\left(\beta\frac{v_l}{v_r}\right)^n G_1^{\prime 1}\left[-n\frac{2c}{v_r}l_0+x+v_l t\right]\right\}^2\mathrm{d}x \tag{54}$$

Taking the derivative of Eqs. (49) to (54) yields

$$\frac{\mathrm{d}E_{F_1^n(t)}}{\mathrm{d}t}=\rho c^2(\beta\frac{v_l}{v_r})^{2(n-1)}[-v_r(F_1^{1\prime}((n-1)\frac{2cl_0}{v_l}+x-v_r t))^2]_{x_1}^{x_2} \tag{55}$$

$$\frac{\mathrm{d}E_{F_2^n(t)}}{\mathrm{d}t}=\rho c^2(\frac{v_l}{v_r})^2(\beta\frac{v_l}{v_r})^{2(n-1)}[-v_r(G_1^{1\prime}(-(n-1)\frac{2cl_0}{v_r}-\frac{v_l}{v_r}(x-v_r t)))^2]_{x_1}^{x_2} \tag{56}$$

$$\frac{\mathrm{d}E_{F_3^n(t)}}{\mathrm{d}t}=\rho c^2(\beta\frac{v_l}{v_r})^{2n}[-v_r(F_1^{1\prime}(n\frac{2cl_0}{v_l}+x-v_r t))^2]_{x_1}^{x_2} \tag{57}$$

$$\frac{\mathrm{d}E_{G_1^n(t)}}{\mathrm{d}t}=\rho c^2(\beta\frac{v_l}{v_r})^{2(n-1)}[v_l(G_1^{1\prime}(-(n-1)\frac{2cl_0}{v_r}+x+v_l t))^2]_{x_1}^{x_2} \tag{58}$$

$$\frac{\mathrm{d}E_{G_2^n(t)}}{\mathrm{d}t}=\rho c^2(\frac{v_r}{v_l})^2(\beta\frac{v_l}{v_r})^{2n}[v_l(F_1^{1\prime}(n\frac{2cl_0}{v_l}-\frac{v_r}{v_l}x-v_r t))^2]_{x_1}^{x_2} \tag{59}$$

$$\frac{\mathrm{d}E_{G_3^n(t)}}{\mathrm{d}t}=\rho c^2(\beta\frac{v_l}{v_r})^{2n}[v_l(G_1^{1\prime}(-n\frac{2cl_0}{v_r}+x+v_l t))^2]_{x_1}^{x_2} \tag{60}$$

Eqs. (55) to (60) are the expressions of the energy gradient for a control volume in terms of the waves.

Likewise, the total energy in the $n^{th}$ cycle can be expressed separately in three time intervals of this cycle as follows.

### 4.1.1 $(n\text{-}1)T < t < (n\text{-}1)T + t_a$

The total energy is the combination of the energy of these four propagating waves $F_1^n$, $F_2^n$, $G_1^n$, $G_2^n$ in the $n^{th}$ cycle and the energy associated with the rigid-body translation of the traveling string. So the energy and its gradient for the string can be written as

$$\begin{aligned}E^n\left(t\right)=&E_{F_1^n}\left(t\right)_{x_1=v_r(t-(n-1)T),x_2=l_0}+E_{F_2^n}\left(t\right)_{x_1=0,x_2=v_r(t-(n-1)T)}\\&+E_{G_1^n}\left(t\right)_{x_1=0,x_2=l_0-v_l(t-(n-1)T)}+E_{G_2^n}\left(t\right)_{x_1=l_0-v_l(t-(n-1)T),x_2=l_0}+\frac{1}{2}\rho v^2 l_0\end{aligned} \tag{61}$$

where $E_{F_1^n}\left(t\right)$, $E_{F_2^n}\left(t\right)$, $E_{G_1^n}\left(t\right)$ and $E_{G_2^n}\left(t\right)$ are the energy of $F_1$, $F_2$, $G_1$ and $G_2$ in the $n^{th}$ cycle, respectively.

$$\frac{\mathrm{d}E^n(t)}{\mathrm{d}t}=\frac{\mathrm{d}E_{F_1^n}(t)}{\mathrm{d}t}\Big|_{\substack{x_2=l_0\\ x_1=v_r(t-(n-1)T)}}+\frac{\mathrm{d}E_{F_2^n}(t)}{\mathrm{d}t}\Big|_{\substack{x_2=v_r(t-(n-1)T)\\ x_1=0}}$$
$$+\frac{\mathrm{d}E_{G_1^n}(t)}{\mathrm{d}t}\Big|_{\substack{x_2=l_0-v_l(t-(n-1)T)\\ x_1=0}}+\frac{\mathrm{d}E_{G_2^n}(t)}{\mathrm{d}t}\Big|_{\substack{x_2=l_0\\ x_1=l_0-v_l(t-(n-1)T)}} \tag{62}$$

As one can see from Eq. (43), the energy gradient for the control volume is only related with the boundaries. So Eq. (62) can be simplified as follows.

$$\frac{\mathrm{d}E^n(t)}{\mathrm{d}t}=\frac{\mathrm{d}E_{F_1^n}(t)}{\mathrm{d}t}\Big|_{x=l_0}-\frac{\mathrm{d}E_{F_2^n}(t)}{\mathrm{d}t}\Big|_{x=0}-\frac{\mathrm{d}E_{G_1^n}(t)}{\mathrm{d}t}\Big|_{x=0}+\frac{\mathrm{d}E_{G_2^n}(t)}{\mathrm{d}t}\Big|_{x=l_0} \tag{63}$$

### 4.1.2 ***(n-1)T + t_a < t < (n-1)T + t_b***

The energy is due to the waves $G_1$, $G_2$, $G_3$ and $F_2$ in the $n^{th}$ cycle. The total energy expression and its gradient for control volume can be written as

$$E^n(t)=E_{G_1^n}(t)_{x_1=0,x_2=l_0-v_l(t-(n-1)T)}+E_{G_2^n}(t)_{x_1=l_0-v_l(t-(n-1)T),x_2=\frac{2cl_0}{v_r}-v_l(t-(n-1)T)}+$$
$$E_{G_3^n}(t)_{x_1=\frac{2cl_0}{v_r}-v_l(t-(n-1)T),x_2=l_0}+E_{F_2^n}(t)_{x_1=0,x_2=l_0}+\frac{1}{2}\rho v^2 l_0 \tag{64}$$

$$\frac{\mathrm{d}E^n(t)}{\mathrm{d}t}=\frac{\mathrm{d}E_{G_1^n}(t)}{\mathrm{d}t}\Big|_{\substack{x_2=l_0-v_l(t-(n-1)T)\\ x_1=0}}+\frac{\mathrm{d}E_{G_2^n}(t)}{\mathrm{d}t}\Big|_{\substack{x_2=\frac{2cl_0}{v_r}-v_l(t-(n-1)T)\\ x_1=l_0-v_l(t-(n-1)T)}}+$$
$$\frac{\mathrm{d}E_{G_3^n}(t)}{\mathrm{d}t}\Big|_{\substack{x_2=l_0\\ x_1=\frac{2cl_0}{v_r}-v_l(t-(n-1)T)}}+\frac{\mathrm{d}E_{F_2^n}(t)}{\mathrm{d}t}\Big|_{\substack{x_2=l_0\\ x_1=0}} \tag{65}$$
$$=-\frac{\mathrm{d}E_{G_1^n}(t)}{\mathrm{d}t}\Big|_{x=0}+\frac{\mathrm{d}E_{G_3^n}(t)}{\mathrm{d}t}\Big|_{x=l_0}+\frac{\mathrm{d}E_{F_2^n}(t)}{\mathrm{d}t}\Big|_{\substack{x_2=l_0\\ x_1=0}}$$

### 4.1.3 ***(n-1)T + t_b < t < nT***

The energy is due to the waves $F_2$, $F_3$, $G_2$, and $G_3$ in the $n^{th}$ cycle. The total energy expression and its gradient for control volume can be written as

$$E^n(t)=E_{F_2^n}(t)_{x_1=v_r(t-(n-1)T)-\frac{v_r}{v_l}l_0,x_2=l_0}+E_{F_3^n}(t)_{x_1=0,x_2=v_r(t-(n-1)T)-\frac{v_r}{v_l}l_0}$$
$$+E_{G_2^n}(t)_{x_1=0,x_2=\frac{2c}{v_r}l_0-v_l(t-(n-1)T)}+E_{G_3^n}(t)_{x_1=\frac{2c}{v_r}l_0-v_l(t-(n-1)T),x_2=l_0}+\frac{1}{2}\rho v^2 l_0 \tag{66}$$

$$\frac{\mathrm{d}E^n(t)}{\mathrm{d}t}=\frac{\mathrm{d}E_{F_2^n}(t)}{\mathrm{d}t}\Big|_{\substack{x_2=l_0\\ x_1=v_r(t-(n-1)T)-\frac{v_r}{v_l}l_0}}+\frac{\mathrm{d}E_{F_3^n}(t)}{\mathrm{d}t}\Big|_{\substack{x_2=v_r(t-(n-1)T)-\frac{v_r}{v_l}l_0\\ x_1=0}}$$
$$+\frac{\mathrm{d}E_{G_2^n}(t)}{\mathrm{d}t}\Big|_{\substack{x_2=\frac{2c}{v_r}l_0-v_l(t-(n-1)T)\\ x_1=0}}+\frac{\mathrm{d}E_{G_3^n}(t)}{\mathrm{d}t}\Big|_{\substack{x_2=l_0\\ x_1=\frac{2c}{v_r}l_0-v_l(t-(n-1)T)}} \tag{67}$$
$$=\frac{\mathrm{d}E_{F_2^n}(t)}{\mathrm{d}t}\Big|_{x=l_0}-\frac{\mathrm{d}E_{F_3^n}(t)}{\mathrm{d}t}\Big|_{x=0}-\frac{\mathrm{d}E_{G_2^n}(t)}{\mathrm{d}t}\Big|_{x=0}+\frac{\mathrm{d}E_{G_3^n}(t)}{\mathrm{d}t}\Big|_{x=l_0}$$

So the total energy of the traveling string can be calculated using the initial conditions and Eqs. (61), (64) and (66).

### 4.2 Vibration suppression at boundaries

When $\beta = 0$, after the first cycle ($n \geq 2$), the energy gradient for the control volume is equal to zero from Eqs. (55) to (60), which means the traveling string just has axial kinetic energy and it does not vibrate. Hence an optimal damping expression for the total elimination of vibration is as follows.

$$\eta_{opt} = \frac{P}{v_r} = \frac{\rho c^2}{c+v} \tag{68}$$

On one hand, the optimal damping can be validated by [24] which shows optimality and effectiveness of the control method by a finite difference scheme. On the other hand, the optimal damping can be explained from the boundary reflection relationships in Eqs. (12) and (11). Substituting $\beta$ =0 into Eq. (12), yields

$$G'\left(l_0 + v_l t\right)=0 \tag{69}$$

which means the response of $G(l_0+v_l t)$ at the damping boundary is a constant after the first cycle. Thus $G(x+v_l t)$ always equals $G_1(l_0)$ which can be obtained by Eq. (19). From Eq. (11), when $G$ reaches the fixed boundary, the reflected wave $F$ is always equal to a constant which is opposite in magnitude and phase to $G$. As a result, the response equals zero, which is the same as mentioned above from the view of energy.

## 5. Simulations and discussions

**Table 1** Chosen parameters for the simulations

| $l_0$ | $\rho$ | $P$ | $v$ | $A_0$ |
|---|---|---|---|---|
| 3m | 0.06kg/m | 5N | 0.3$c$ | 0.01m |

The parameters given in Table 1 were used for the subsequent simulations. Other parameters are not independent and can be calculated by these basic parameters.
the initial conditions for displacement and velocity are

$$\begin{cases} \phi(x) = \dfrac{16\times A_0 x^2 (l_0 - x)^2}{{l_0}^4} \\ \psi(x) = 0 \end{cases} \tag{70}$$

### 5.1 The process of traveling waves reflection

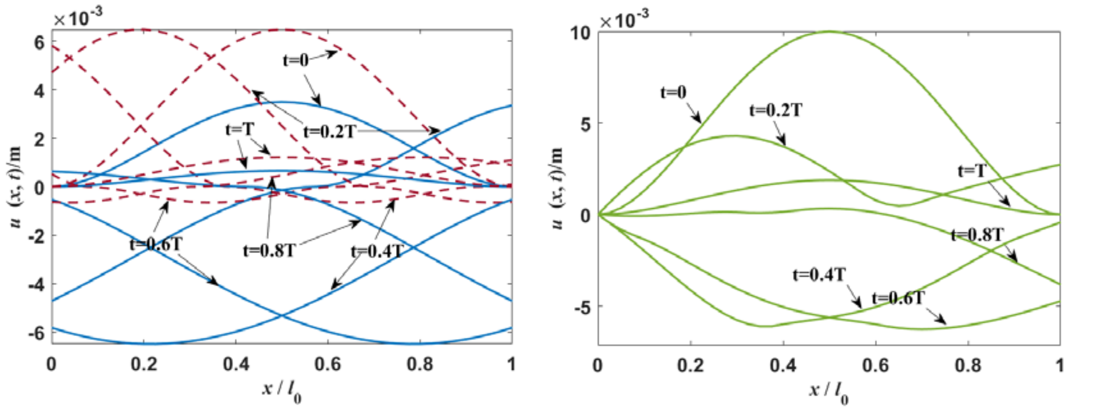


(a) (b)

**Fig. 4** Displacement responses for the first propagating cycle with boundary damping coefficient $\eta$=0.7 Ns/m. (a) shows the right and the left propagating waves at different moment in the first cycle; (b) shows the real displacement. The curves are identified by: —— the right propagating wave, - - - the left propagating wave, —— the real displacement.

As an example, the process of propagating waves reflection is plotted in Fig. 4. At the fixed boundary, the reflected wave is exactly the odd, periodic extension ([29]) of the incident wave. The odd extension can be explained by Eq.(11). However, the reflection relationship at the dashpot boundary, which can't be obtained by the odd extension, is more complex and suited to Eq.(12).

## 5.2 Displacement responses

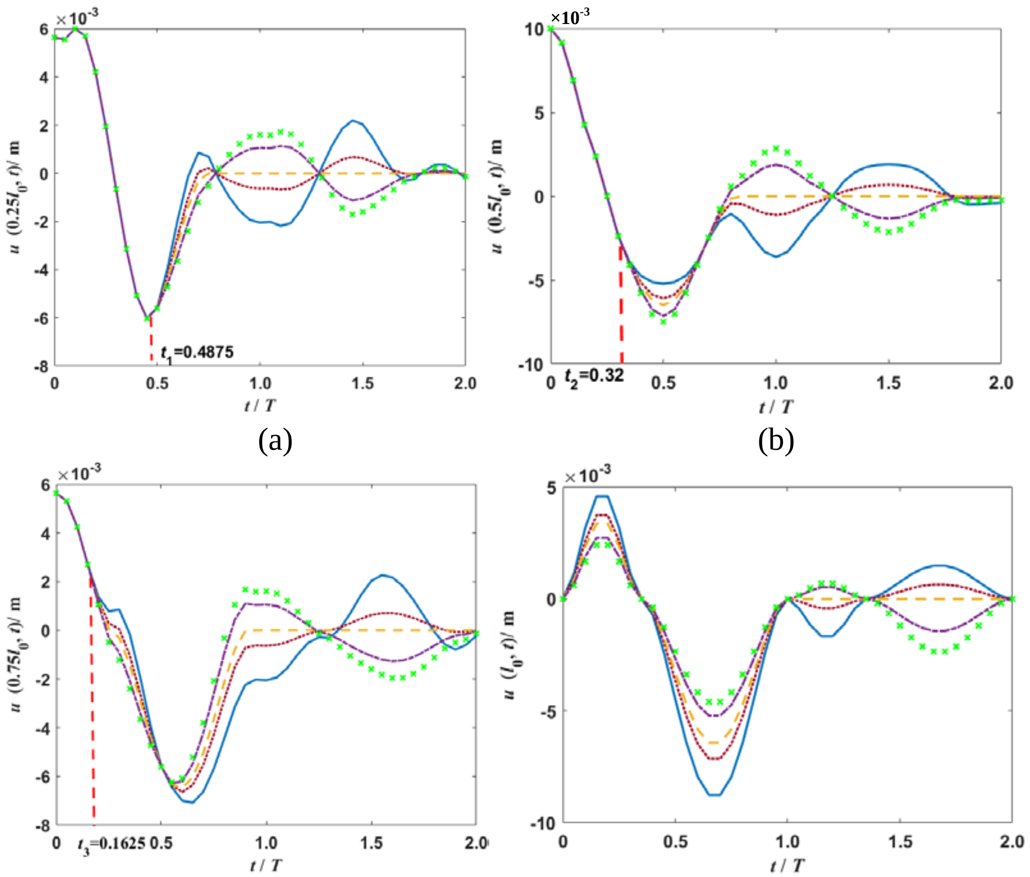

(c) (d)

**Fig. 5** Displacement responses of transverse free vibration with fixed_dashpot boundary condition and the initial conditions of Eq. (67) over two cycles at location of (a) $x = 0.25l_0$, (b) $x = 0.5l_0$, (c) $x = 0.75l_0$ and (d) $x = l_0$, respectively. The curves are identified by:—— $\eta = 0.1$ Ns/m, ········ $\eta = 0.3$ Ns/m, - - - - $\eta = 0.4213$ Ns/m (the optimal value of the boundary damping $\eta_{opt}$), —·— $\eta = 0.7$ Ns/m and × × × × × $\eta = 0.9$ Ns/m.

Fig. 5 demonstrates the response of axially traveling string for the fixed_dashpot boundary conditions over two cycles. The displacement responses of transverse free vibration are shown at selected fixed coordinate positions ($x = 0.25\ l_0$, $0.5\ l_0$, $0.75\ l_0$ and $l_0$) are given, for different levels of viscous damping at the right hand boundary ($\eta$ = 0.1 Ns/m, 0.3 Ns/m, 0.493 Ns/m, 0.7 Ns/m and 0.9 Ns/m).

From Fig. 5 (a) to (d), after the first cycle, the reduction of vibration is most obvious for the optimal value of the boundary damping $\eta_{\text{opt}}$. After the first cycle, the axially traveling string does not have vibration because the energy gradient is zero with $\eta = \eta_{\text{opt}}$, which is mentioned in section 4.2. In Fig. 5 (a) to (c), five curves overlap completely in the time interval of $(0, t_1)$, $(0, t_2)$ and $(0, t_3)$ respectively, because the reflected waves, i.e. $G_2$ that was attenuated at the right boundary have not yet reached the respective coordinate position ($x = 0.25\ l_0$, $x = 0.5\ l_0$ and $x = 0.75\ l_0$). Here the dimensionless times are $t_1 = 0.75\ l_0 / (Tv_l) = 0.4875$, $t_2 = 0.5\ l_0 / (Tv_l) = 0.32$ and $t_3 = 0.25\ l_0 / (Tv_l) = 0.1625$.

### 5.3 Energy simulations

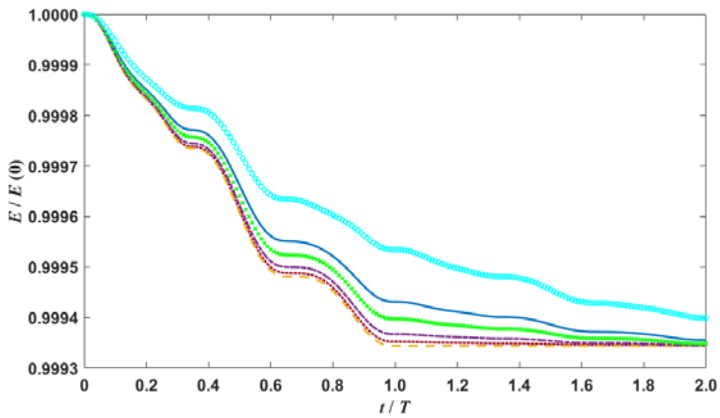


**Fig. 6** The total transverse free vibration energy of an axially traveling string with fixed_dashpot boundary conditions over two cycles. Curves are identified by the level of the viscous damping constant: ○ ○ ○ ○ ○ $\eta = 0$ Ns/m, —— $\eta = 0.1$ Ns/m, ········ $\eta = 0.3$ Ns/m, - - - - $\eta = 0.4213$ Ns/m (the optimal value of the boundary damping $\eta_{\text{opt}}$), —·— $\eta = 0.7$ Ns/m, × × × × × $\eta = 0.9$ Ns/m.

Fig. 6 shows the total transverse free vibration energy of an axially traveling string with fixed_dashpot boundary conditions over multiple cycles for different damping levels compared. The situation of $\eta = 0$ Ns/m corresponds to fixed-free boundaries. Since the tension of $P$ acting on the string at the left fixed end is opposite to the traveling direction of the string, the left boundary does negative work on the string and the free end at the right end does no work on the string, so the system energy is always decreasing with time. The rate for the decrease in the energy fluctuates with time and the total energy is close to zero after two periods, but never equal to zero since the existence of kinetic energy for axial motion. When $0 < \eta < \eta_{opt}$, the energy of the traveling string system decreases in the cycle, and the larger that the viscous damping is, the more rapid is the attenuation. When $\eta > \eta_{opt}$, the larger that the viscous damping is, the less rapid is the attenuation.

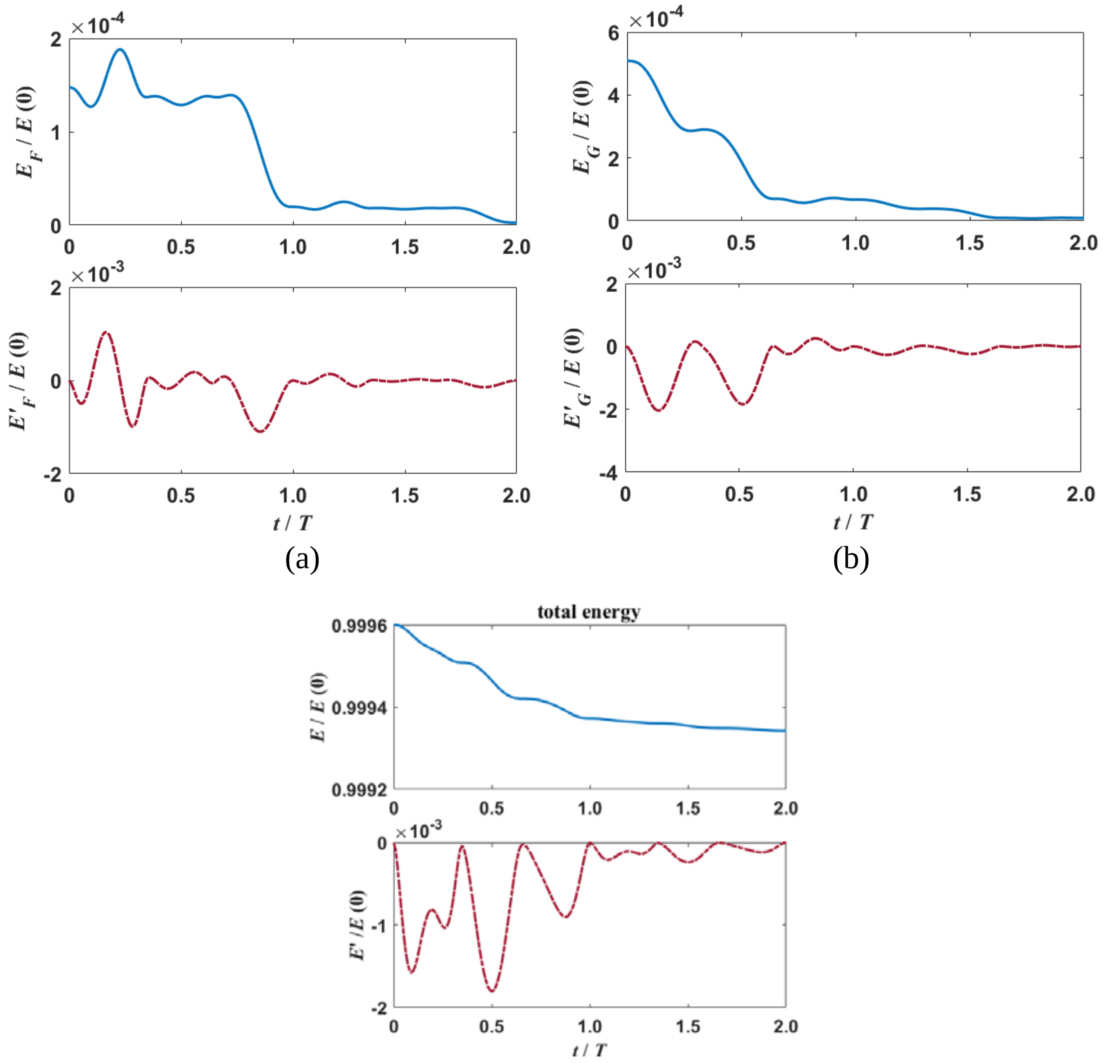


(a) (b) (c)

**Fig. 7** The energy and energy gradient for the control volume over multiple cycles where $\eta$ = 0.1 Ns/m. The energy and energy gradient for the control volume are identified by: —— energy; -·-· energy gradient for the control volume. (a) is for the right-propagating wave *F*, (b) is for the left-propagating wave *G* and (c) is for the total energy

Fig. 7 shows the total energy and its gradient, as well as the energy in the right and left propagating waves *F* and *G* respectively. The energy in the two propagating waves does not always keep decreasing, though the general trend is down.

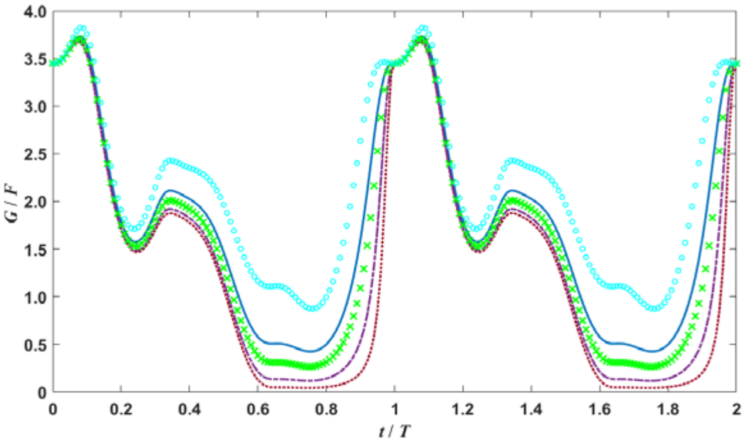


**Fig. 8** The energy ratio of the left-propagating wave $G$ to the right-propagating wave $F$ for different levels of boundary viscous damping. Curves are identified by the level of the viscous damping constant: ○ ○ ○ ○ ○ $\eta$ = 0 Ns/m, —— $\eta$ = 0.1 Ns/m, ········ $\eta$ = 0.3 Ns/m, —·— $\eta$ = 0.7 Ns/m, × × × × × $\eta$ = 0.9 Ns/m.

Fig. 8 shows the energy ratio of the left-propagating wave $G$ to the right-propagating wave $F$. With arbitrary viscous damping constant besides $\eta_{\text{opt}}$, the energy ratio of $G$ to $F$ goes back to the original value after an integer cycle of propagating around the string between the boundaries. Combining Eq. (31) and Eq. (32), the same value for the energy ratio of $G$ to $F$ at the beginning of every cycle can be calculated

$$\frac{\int_0^{l_0}\rho c^2[G_1^{n\prime}(x+v_l(n-1)t)]^2\mathrm{d}x}{\int_0^{l_0}\rho c^2[F_1^{n\prime}(x-v_r(n-1)t)]^2\mathrm{d}x}=\frac{\int_0^{l_0}\rho c^2[(\beta\frac{v_l}{v_r})^{n-1}G_1^{1\prime}(x)]\mathrm{d}x}{\int_0^{l_0}\rho c^2[(\beta\frac{v_l}{v_r})^{n-1}F_1^{1\prime}(x)]\mathrm{d}x}=\frac{\int_0^{l_0}\rho c^2[\frac{v_r}{2c}\phi'(x)+\frac{1}{2c}\varphi(x)]\mathrm{d}x}{\int_0^{l_0}\rho c^2[\frac{v_l}{2c}\phi'(x)-\frac{1}{2c}\varphi(x)]\mathrm{d}x}=3.3955 \tag{71}$$

The energy ratio of $G$ to $F$ is cyclical, even though the sum of energy for $G$ and $F$ keeps changing.

For studying the inflow and outflow of power at the boundaries, the gradient of the propagating wave energy is presented in the following figures.

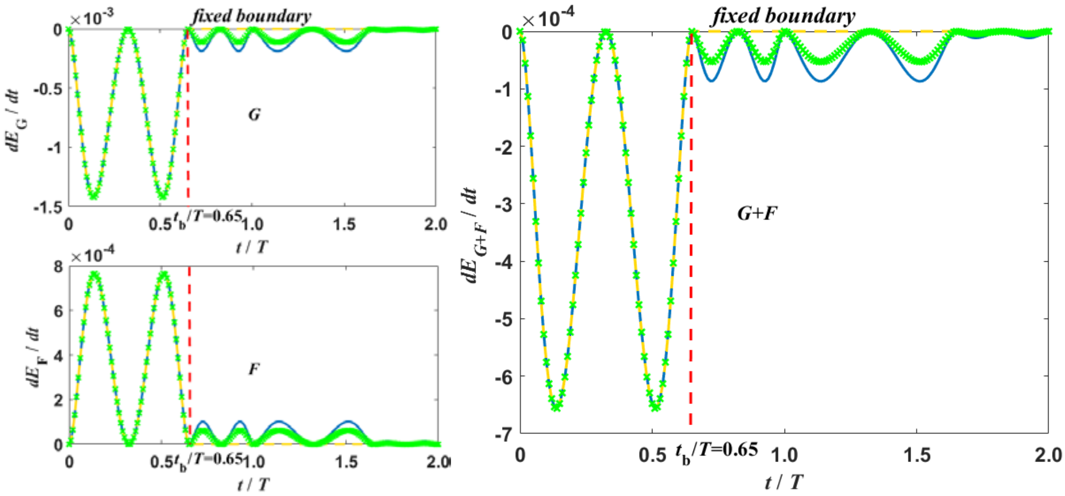


(a) (b)

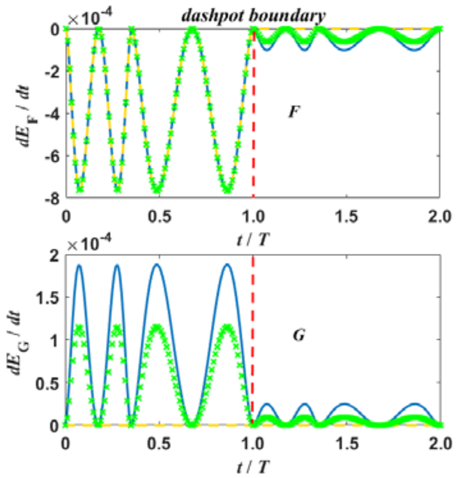


(c)

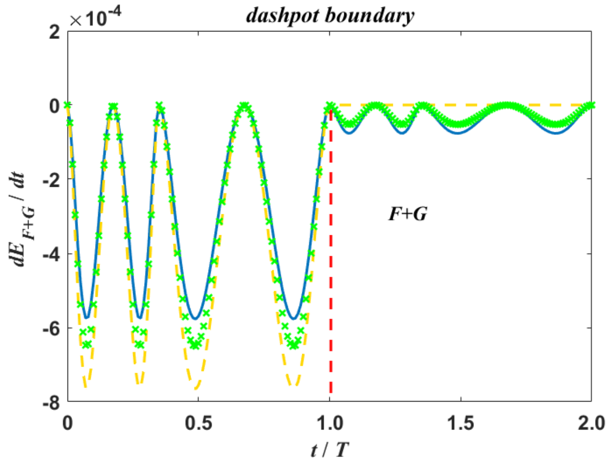


(d)

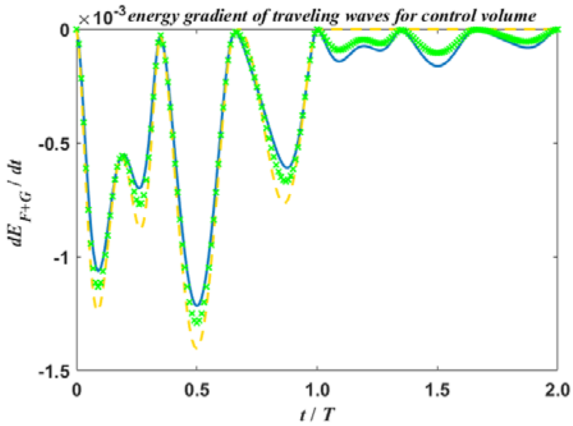


(e)

**Fig. 9** The gradient of the propagating wave energy at boundaries in the multiple cycles ($v$ = 0.3$c$). Here, the energy gradient is for the *control volume*. (a) is for the left-propagating wave $G$ and the right-propagating wave $F$ at upstream (fixed boundary), (b) is for total traveling wave ($F$ + $G$) at upstream, (c) is for $F$ and $G$ at downstream (dashpot boundary), (d) is for total traveling wave ($F$ + $G$) at downstream and (e) is for total energy gradient of traveling wave ($F$ + $G$). Curves are identified by the level of the viscous damping constant: —— $\eta$ = 0.1 Ns/m, - - - - $\eta$ = 0.4213 Ns/m (the optimal value of the boundary damping $\eta_{\text{opt}}$), × × × × × $\eta$ = 0.9 Ns/m.

Fig. 9 demonstrates that the incident wave has outflow of energy and the reflected wave has inflow of power at both boundaries. As time progresses, the amplitude of the energy gradient for left and right propagating waves decreases.

As Fig. 9 (a) and (b) show, in the first cycle before $t_b/T_0$=0.65, the curves are overlapping because $\frac{\mathrm{d}E_{F_2^1(t)}}{\mathrm{d}t}\Big|_{x=0}$ and $\frac{\mathrm{d}E_{G_1^1(t)}}{\mathrm{d}t}\Big|_{x=0}$ are not related to $\eta$ as well as $\beta$ since $n$ = 1, which was obtained by Eq. (55) and Eq. (58). That means they do not change, though the damping value changes downstream. After the first cycle, the closer the damping value is to $\eta_{\text{opt}}$, the smaller the value of power inflow or outflow.

From inspection of Fig. 9 (c) to (d), similar conclusions can be drawn. In the first cycle, curves are overlapping for wave $F$ because $\frac{\mathrm{d}E_{F_1^1(t)}}{\mathrm{d}t}\Big|_{x=l_0}$ and $\frac{\mathrm{d}E_{F_2^1(t)}}{\mathrm{d}t}\Big|_{x=l_0}$ are not related to $\eta$, which can be obtained from Eq. (55) and Eq. (56). While curves are not overlapping for wave $G$, because of $\frac{\mathrm{d}E_{G_2^1(t)}}{\mathrm{d}t}\Big|_{x=l_0}$ and $\frac{\mathrm{d}E_{G_3^1(t)}}{\mathrm{d}t}\Big|_{x=l_0}$ are related to $\eta$ which can be obtained from Eq. (59) and Eq. (60). In particular as shown in Fig. 9 (c), $\frac{\mathrm{d}E_{G(t)}}{\mathrm{d}t}\Big|_{x=l_0}$ equal zeros for $\eta = \eta_{\mathrm{opt}}$ identified by the yellow dash line, which means the optimal damping dissipates all incident energy.

Shifting the focus to the energy gradient for the *system*, the results differ from the above energy gradient for the *control volume* can be shown as follows.

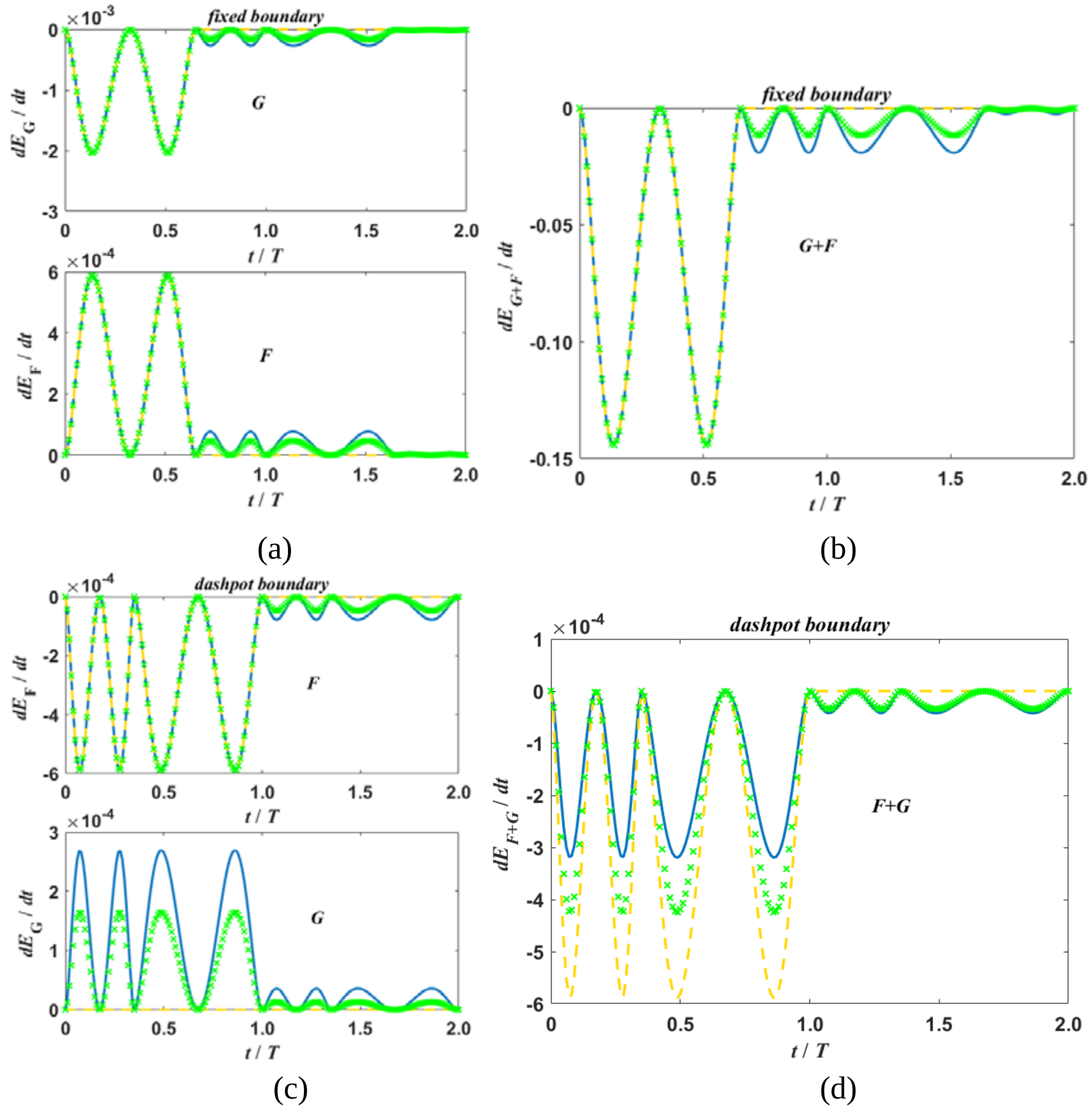


(a) (b)

(c) (d)

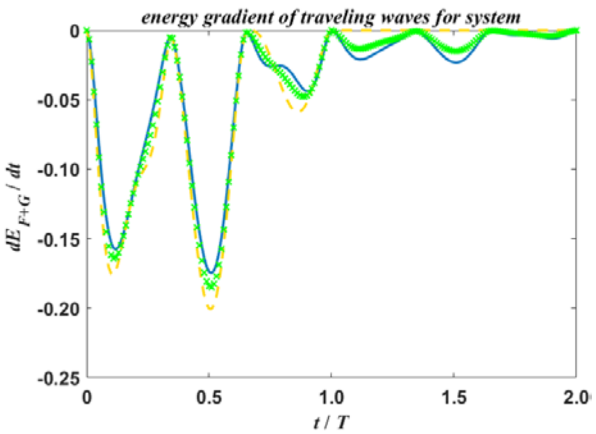


(e)

**Fig. 10** The energy gradient for the propagating wave at boundaries over multiple cycles ($v$ = 0.3$c$). Here, the energy gradient is for the *system*. (a) is the energy gradient for the left-propagating wave $G$ and the right-propagating wave $F$ at upstream (fixed boundary), (b) is the energy gradient for total traveling wave ($F + G$) at upstream, (c) is the energy gradient for $F$ and $G$ at downstream (dashpot boundary), (d) is the energy gradient for total traveling wave ($F + G$) at the downstream end and (e) is the energy gradient for total energy gradient of traveling wave ($F + G$). Curves are identified by the level of the viscous damping constant: —— $\eta$ = 0.1 Ns/m, - - - - $\eta$ = 0.4213 Ns/m (the optimal value of the boundary damping $\eta_{\text{opt}}$), × × × × × $\eta$ = 0.9 Ns/m.

Fig. 10 and Fig. 9 are similar because the expressions are similar, which can also be obtained from Eq. (47) and Eq. (43). Particularly, in Fig. 10 (e), the energy gradient of system equals the rate of work done by boundaries.

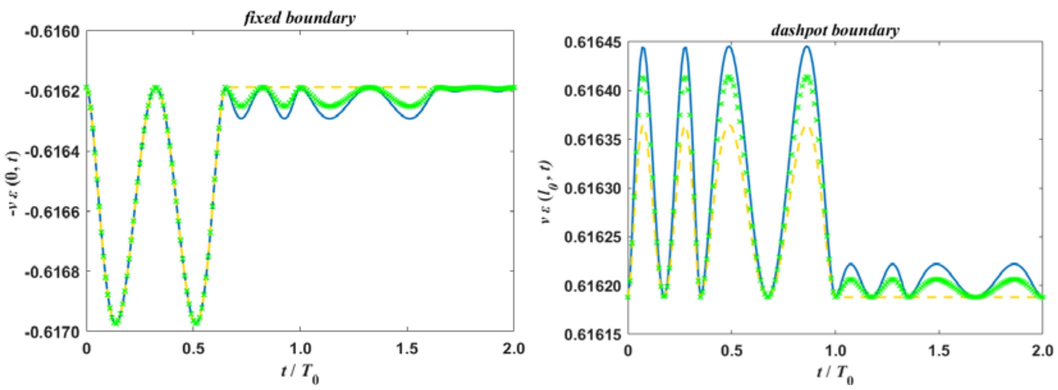


(a) (b)

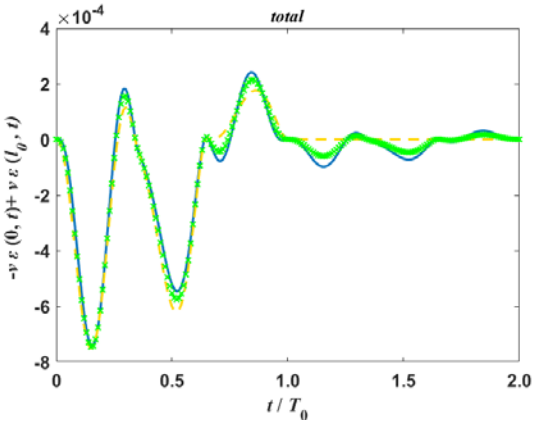


(c)

**Fig. 11** The net flow rate of energy out of control volume by the flow of the string material. (a) is for the upstream, (b) is for the downstream and (c) is the superposition of (a) and (b). Curves are identified by the level of the viscous damping constant: —— $\eta$ = 0.1 Ns/m, - - - $\eta$ = 0.4213 Ns/m (the optimal value of the boundary damping $\eta_{opt}$), × × × × × $\eta$ = 0.9 Ns/m.

In Fig. 11 (a) and (b), the inflow and outflow of power always exist, even for the optimal damping value, because the string still has axial kinetic energy even though it doesn't vibrate. Also, the net inflow or outflow rate of energy is $0.5\rho v^3$=0.6162W. Fig. 10 (e) is the superposition of Fig. 9 (e) and Fig. 11 (c) which represents the net flow rate of energy out of control volume caused by the flow of the string material.

Given the excellent performance of the optimal damping boundary in vibration suppression, in engineering practice, the dampers or variable dampers with appropriate damping values can be installed at the boundary of the moving material which can be modeled as a traveling string system to ensure the normal operation of the equipment.

In this paper, there are two kinds of energy gradient examined, namely the energy gradient for the control volume and the system, both of which are shown using the traveling wave method. The reason of using these two perspectives is the complex variation of total mechanical energy which is caused by two sources [22]: the transport of the string through the domain (0, $l_0$) and the rate of work done by the external forces and moments (support forces and damping forces). The Reynolds transport theorem provides a link for energy between the control volume and the system.

### 5.4 Application and verification

A yarn in the textile industry matches the traveling string model closely. According to practical yarn parameters in textile processing, some of the parameters in **Table 1** change as follows: $l_0$=1.6m, $\rho$=0.0002kg/m, $P$=0.005N, $v$=0.81m/s. The initial conditions are the same as Eq. (70). The plots in **Fig. 12** show the displacement responses of the yarn with fixed_dashpot boundary conditions using the proposed method, which are compared with the numerical solutions of a finite element model solved using the Newmark-$\beta$ method [30]. The results of the two methods are consistent with each other. Especially for the optimal damping, both methods show good performance of vibration suppression.

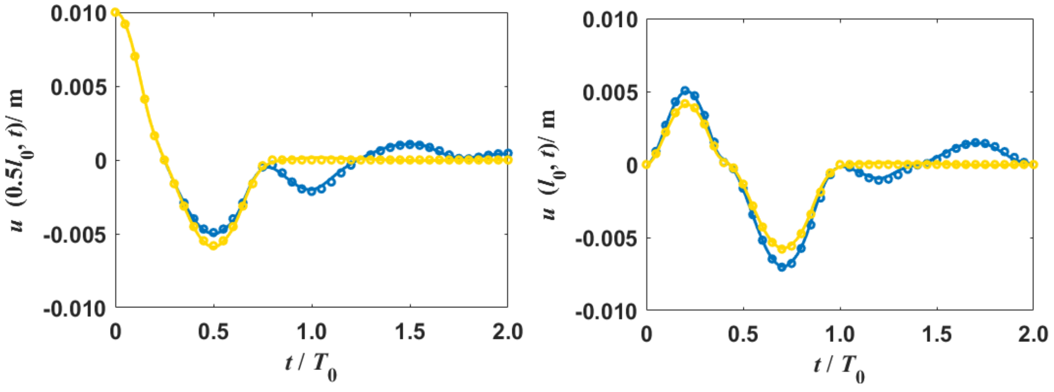


**Fig. 12** Displacement responses at locations of $x$ = 0.5$l_0$ and $x$ = $l_0$ with fixed_dashpot boundary conditions for the first two propagation cycles. Curves are identified by: ——— the Newmark-$\beta$ method with $\eta$=0.00050Ns/m; ○○○○○ the traveling wave method with $\eta$=0.00050Ns/m; ——— the Newmark-$\beta$ method with $\eta$=0.00088Ns/m ( the optimal value of the boundary damping $\eta_{opt}$); and ○○○○○ the traveling wave method with $\eta$=0.00088Ns/m.

## 6. Conclusions

Based on d'Alembert's method and a reflected wave superposition method, the exact solution for a finite traveling string with initial conditions in any cycle can be obtained. As a kind of nonclassical boundary, dashpot boundary is considered. The boundary reflection law is essential and provides an understanding of how waves are reflected by the boundaries. As a result, research into identifying an optimal value of the boundary damping provides a basis for active vibration control of axially traveling materials with dissipative boundaries.

For the greatest vibration attenuation, this study shows that having a higher level of viscous damping at the corresponding boundary is not necessarily any better. There is an optimal value for the boundary damping, which is system dependent, after the first cycle. This was identified by numerical simulations of either the displacement response or energy. In the form of traveling waves, the energy ratio of the left-propagating wave to the right-propagating wave goes back to the original value cyclically after an integer number of cycles. For the system, the gradient of energy has a clear physical interpretation as it relates the gradient of the vibrational energy with the rate of work (power) done by forces at the two boundaries.

## 7. Declaration of Competing Interest

The authors declare that they have no known competing financial interests or personal relationships that could have appeared to influence the work reported in this paper.


## 8. Acknowledgments

This work was supported by the National Natural Science Foundation of China [grant numbers 51675150, 51305115 and 11772100].

## Reference

[1] L. Li, I. Kao, Damped Vibration Response of An Axially Moving Wire Subject to An Oscillating Boundary Condition and the Application to Slurry Wiresaws, J. Vib. Acoust., 143 (2021). https://doi.org/10.1115/1.4049269.

[2] P.T. Pham, K.S. Hong, Dynamic models of axially moving systems: A review, Nonlinear Dyn., 100 (2020) 315-349. http://doi.org/10.1007/s11071-020-05491-z.

[3] S.Y. Lee, J.C.D. Mote, A generalized treatment of the energetics of translating continua, part I: Strings and second order tensioned pipes, J. Sound Vib., 204 (1997) 735-753. https://doi.org/10.1006/jsvi.1996.0946.

[4] K.S. Hong, P.T. Pham, Control of Axially Moving Systems: A Review, Int. J. Control Autom. Syst., 17 (2019) 2983-3008. http://doi.org/10.1007/s12555-019-0592-5.

[5] N.V. Gaiko, W.T. van Horssen, On wave reflections and energetics for a semi-infinite traveling string with a nonclassical boundary support, J. Sound Vib., 370 (2016) 336-350. http://doi.org/10.1016/j.jsv.2016.01.040.

[6] E.W. Chen, Q. Luo, N.S. Ferguson, Y.M. Lu, A reflected wave superposition method for vibration and energy of a travelling string, J. Sound Vib., 400 (2017) 40-57. http://doi.org/10.1016/j.jsv.2017.03.046.

[7] E.W. Chen, Y.Q. He, K. Zhang, H.Z. Wei, Y.M. Lu, A superposition method of reflected wave for moving string vibration with nonclassical boundary, J. Chin. Inst. Eng., 42 (2019) 327-332. http://doi.org/10.1080/02533839.2019.1584735.

[8] E.W. Chen, K. Zhang, N.S. Ferguson, J. Wang, Y.M. Lu, On the reflected wave superposition method for a travelling string with mixed boundary supports, J. Sound Vib., 440 (2019) 129-146. https://doi.org/10.1016/j.jsv.2018.10.001.

[9] E.W. Chen, J.F. Yuan, N.S. Ferguson, K. Zhang, W.D. Zhu, Y.M. Lu, H.Z. Wei, A wave solution for energy dissipation and exchange at nonclassical boundaries of a traveling string, Mech. Syst. Sig. Process., 150 (2021) 107272. https://doi.org/10.1016/j.ymssp.2020.107272.

[10] J.T.S. Wang, C.C. Lin, Dynamic analysis of generally supported beams using fourier series, J. Sound Vib., 196 (1996) 285-293. https://doi.org/10.1006/jsvi.1996.0484.

[11] H. Chung, Free vibration analysis of circular cylindrical shells, J. Sound Vib., 74 (1981) 331-350. https://doi.org/10.1016/0022-460X(81)90303-5.

[12] N.V. Gaiko, W.T. van Horssen, On transversal oscillations of a vertically translating string with small time-harmonic length variations, J. Sound Vib., 383 (2016) 339-348. https://doi.org/10.1016/j.jsv.2016.07.019.

[13] R.A. Malookani, W.T. van Horssen, On the Vibrations of an Axially Moving String With a Time-Dependent Velocity, ASME 2015 International Mechanical Engineering Congress and Exposition, Volume 4B: Dynamics, Vibration, and Control (2015). https://doi.org/10.1115/IMECE2015-50452.

[14] S. Dehraj, S.H. Sandilo, R.A. Malookani, On applicability of truncation method for damped axially moving string, J. Vibroeng., 22 (2020) 337-352. https://doi.org/10.21595/jve.2020.21192.

[15] R.D. Swope, W.F. Ames, Vibrations of a moving threadline, J. Franklin Inst., 275 (1963) 36-55. https://doi.org/10.1016/0016-0032(63)90619-7.

[16] L. Sirota, Y. Halevi, Extended D'Alembert solution of finite length second order flexible

structures with damped boundaries, Mech. Syst. Sig. Process., 39 (2013) 47-58. https://doi.org/10.1016/j.ymssp.2012.01.006.
[17] E.W. Chen, J. Wang, K. Zhong, Y. Lu, H. Wei, Vibration dissipation of an axially traveling string with boundary damping, J. Vibroeng., 19 (2017) 5780-5795. http://doi.org/10.21595/jve.2017.18651.
[18] J.H. Sällström, B. kesson, Fluid-conveying damped Rayleigh-Timoshenko beams in transverse vibration analyzed by use of an exact finite element part I: Theory, J. Fluids Struct., 4 (1990) 561-572. https://doi.org/10.1016/0889-9746(90)90202-G.
[19] T.B. Benjamin, G.K. Batchelor, Dynamics of a System of Articulated Pipes Conveying Fluid. I. Theory, Proc. R. Soc. London Ser. A-Math. Phys. Eng. Sci., 261 (1961) 457-486. https://doi.org/10.1098/rspa.1961.0090.
[20] D.B. McIver, Hamilton's principle for systems of changing mass, J. Eng. Math., 7 (1973) 249-261. http://doi.org/10.1007/BF01535286.
[21] C.W. Kim, K.S. Hong, H. Park, Boundary control of an axially moving string: actuator dynamics included, J. Mech. Sci. Technol., 19 (2005) 40-50. http://doi.org/10.1007/bf02916103.
[22] A.A. Renshaw, C.D. Rahn, J.A. Wickert, C.D. Mote, Jr., Energy and conserved functionals for axially moving materials, J. Vib. Acoust., 120 (1998) 634-636. http://doi.org/10.1115/1.2893875.
[23] W.D. Zhu, Control volume and system formulations for translating media and stationary media with moving boundaries, J. Sound Vib., 254 (2002) 189-201. http://doi.org/10.1006/jsvi.2001.4055.
[24] S.Y. Lee, C.D. Mote, Jr., Vibration control of an axially moving string by boundary control, J. Dyn. Sys., Meas., Control., 118 (1996) 66-74. http://doi.org/10.1115/1.2801153.
[25] M.H. Ghayesh, H.A. Kafiabad, T. Reid, Sub- and super-critical nonlinear dynamics of a harmonically excited axially moving beam, Int. J. Solids Struct., 49 (2012) 227-243. https://doi.org/10.1016/j.ijsolstr.2011.10.007.
[26] Y. ÇEngel, J.M. Cimbala, Fluid Mechanics: Fundamentals and Applications, fourth ed, McGraw-Hill College, 2017.
[27] W.D. Zhu , J. Ni, Energetics and stability of translating media with an arbitrarily varying length, J. Vib. Acoust., 122 (1999) 295-304. http://doi.org/10.1115/1.1303003.
[28] W.D. Zhu, Vibration and Stability of Time-Dependent Translating Media, Shock Vib. Digest, 32 (2000) 369-379. http://doi.org/10.1177/058310240003200502.
[29] Y.M. Ram, J. Caldwell, Free vibration of a string with moving boundary conditions by the method of distorted images, J. Sound Vib., 194 (1996) 35-47. http://doi.org/10.1006/jsvi.1996.0342.
[30] E.W. Chen, N.S. Ferguson, Analysis of energy dissipation in an elastic moving string with a viscous damper at one end, J. Sound Vib., 333 (2014) 2556-2570. https://doi.org/10.1016/j.jsv.2013.12.024.

## Appendix A: Derivation of the governing equation of motion and boundary conditions

An axially traveling string with two boundaries is a system of changing. The modified Hamilton’s principle for system of changing material is ([20, 24])

$$\delta\int_{t_1}^{t_2}(E_k-E_p)\mathrm{d}t-\int_{t_1}^{t_2}(\rho v(u_t+vu_x)\delta u)\bigg|_0^{l_0}\mathrm{d}t+\int_{t_1}^{t_2}F_\eta\delta u(l_0,t)\mathrm{d}t=0 \tag{A1}$$

where $E_k$ is the kinetic energy, $E_p$ is the potential energy and $F_\eta$ =-$\eta u_t(l_0, t)$ is the damping force.

The expressions of $E_k$ and $E_p$ can be obtained by [9] as follows.

$$E_k=\frac{1}{2}\int_0^{l_0}\rho(v^2+(u_t+vu_x)^2)\mathrm{d}x \tag{A2}$$

$$E_p=\frac{1}{2}\int_0^{l_0}P{u_x}^2\mathrm{d}x \tag{A3}$$

Eq. (A1) is simplified as follows.

$$\begin{aligned}&\delta\int_{t_1}^{t_2}\int_0^{l_0}\frac{1}{2}\rho{u_t}^2\mathrm{d}x\mathrm{d}t+\delta\int_{t_1}^{t_2}\int_0^{l_0}\rho vu_tu_x\mathrm{d}x\mathrm{d}t+\delta\int_{t_1}^{t_2}\int_0^{l_0}\frac{1}{2}(\rho v^2-P){u_x}^2\mathrm{d}x\mathrm{d}t\\&-\int_{t_1}^{t_2}(\rho v(u_t+vu_x)\delta u)\bigg|_0^{l_0}\mathrm{d}t-\int_{t_1}^{t_2}\eta u_t(l_0,t)\delta u(l_0,t)\mathrm{d}t=0\end{aligned} \tag{A4}$$

Appling integration by parts to the first four terms of the left side of Eq. (A4), yields

$$\int_0^{l_0}\rho u_t\delta u\bigg|_{t_1}^{t_2}-\int_{t_1}^{t_2}\rho u_{tt}\delta u\mathrm{d}t\mathrm{d}x \tag{A5}$$

$$\int_0^{l_0}2\rho vu_x\delta u\bigg|_{t_1}^{t_2}-\int_{t_1}^{t_2}2\rho vu_{xt}\delta u\mathrm{d}t\mathrm{d}x \tag{A6}$$

$$\int_{t_1}^{t_2}(\rho v^2-P)u_x\delta u\bigg|_0^{l_0}-\int_0^{l_0}(\rho v^2-P)u_{xx}\delta u\mathrm{d}x\mathrm{d}t \tag{A7}$$

$$-\frac{1}{2}\rho v\delta u\bigg|_0^{l_0}\bigg|_{t_1}^{t_2}-\int_{t_1}^{t_2}\rho v^2u_x\delta u\bigg|_0^{l_0}\mathrm{d}t \tag{A8}$$

Assuming δ$u$=0 for $t$=$t_1$ and $t$=$t_2$, and substituting Eqs. (A5)-(A8) to Eq. (A4), yields

$$\int_0^{l_0}\int_{t_1}^{t_2}-\rho[u_{tt}+2vu_{xt}+(v^2-\frac{P}{\rho})u_{xx}]\delta udtdx+\int_{t_1}^{t_2}[-Pu_x\delta u\bigg|_0^{l_0}-\eta u_t(l_0,t)\delta u(l_0,t)]dt \tag{A9}$$

Since the variation δ$u$ is arbitrary, Eq. (A9) can be satisfied only when the individual terms of Eq. (A9) are equal to zero

$$u_{tt}+2vu_{xt}+(v^2-\frac{P}{\rho})u_{xx}=0 \tag{A10}$$

$$-Pu_x\delta u\bigg|_0^{l_0}-\eta u_t(l_0,t)\delta u(l_0,t)=0 \tag{A11}$$

So the dashpot boundary condition obtained from (A11) in Fig. 1 is

$$\eta u_t\left(l_0,t\right)=-Pu_x\left(l_0,t\right) \tag{A12}$$

and Eq. (A10) is the governing equation of motion.

When $\eta$=0 Ns/m, the boundary condition of the right boundary becomes the free boundary: $u_x(l_0, t)$=0.

Appendix B: Fixed_mass-dashpot-spring boundaries case

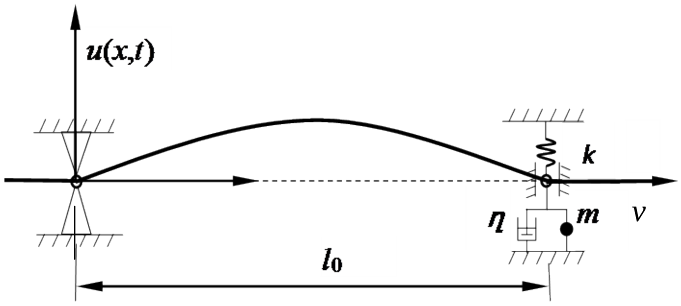

Fig. 13 Traveling string with fixed_ mass-dashpot-spring boundaries.

The mass-dashpot-spring boundary condition in Fig. 13 is

$$mu_{tt}(l_0,t)+ku(l_0,t)+\eta u_t(l_0,t)+Pu_x(l_0,t) \tag{B1}$$

where $k$ is the stiffness of the spring, and $m$ is the mass at the right boundary. The boundary reflection relationship of the right hand boundary is

$$G''(s)+2\alpha\beta G'(s)+\alpha^2 G(s)=R(s) \tag{B2}$$

where $R(s)=F''(\frac{2cl_0-v_r s}{v_l})(-\frac{{v_r}^2}{{v_l}^2})+F'(\frac{2cl_0-v_r s}{v_l})(\frac{\eta v_r-P}{m{v_l}^2})+F(\frac{2cl_0-v_r s}{v_l})(\frac{-k}{m{v_l}^2})$ , $s=l_0+v_l t$ , $\alpha=\sqrt{\frac{k}{m{v_l}^2}}$ , $\beta=\frac{\eta v_l+P}{2v_l\sqrt{mk}}$. The complex boundary conditions lead to a more complex recursive process. Therefore, the recursive formulas for the mass-dashpot-spring boundary reflected waves are given here only instead of response results, and the process of response calculation can be referred to the case of fixed_dashpot boundaries in the main text.

Assume that

$$\mu_{1,2}=\begin{cases}\alpha(-\beta\pm\sqrt{\beta^2-1}) & ,\beta>1\\ -\alpha\beta & ,\beta=1\\ \alpha(-\beta\pm i\sqrt{1-\beta^2}) & ,\beta<1\end{cases} \tag{B3}$$

Following results are for the case of $\beta\neq 1$.

$$G_2{}^n(s)=\frac{\int_{l_0+v_l(n-1)T}^{s}(e^{\mu_2(s-x)}-e^{\mu_1(s-x)})R_1{}^n(x)\mathrm{d}x}{\mu_2-\mu_1}+C_3e^{\mu_1 s}+C_4e^{\mu_2 s} \tag{B4}$$

Here, $R_1{}^n(x)=-\frac{{v_r}^2}{{v_l}^2}F_1{}^{n''}(\frac{2cl_0-v_r x}{v_l})+\frac{\eta v_r-P}{m{v_l}^2}F_1{}^{n'}(\frac{2cl_0-v_r x}{v_l})-\frac{k}{m{v_l}^2}F_1{}^n(\frac{2cl_0-v_r x}{v_l})$,

$$\begin{cases}G_2{}^n(l_0+v_l(n-1)T)=G_1{}^n(l_0+v_l(n-1)T)\\ G_2{}^{n'}(l_0+v_l(n-1)T)=G_1{}^{n'}(l_0+v_l(n-1)T)\end{cases},\quad \begin{cases}C_3=\dfrac{G_1{}^{n'}(l_0+v_l(n-1)T)-\mu_2G_1{}^n(l_0+v_l(n-1)T)}{e^{\mu_1(l_0+v_l(n-1)T)}(\mu_1-\mu_2)}\\ C_4=\dfrac{G_1{}^{n'}(l_0+v_l(n-1)T)-\mu_1G_1{}^n(l_0+v_l(n-1)T)}{e^{\mu_2(l_0+v_l(n-1)T)}(\mu_2-\mu_1)}\end{cases}$$

$$G_3{}^n(s)=\frac{\int_{l_0+v_l(t_a+(n-1)T)}^{s}(e^{\mu_2(s-x)}-e^{\mu_1(s-x)})R_2{}^n(x)\mathrm{d}x}{\mu_2-\mu_1}+C_3e^{\mu_1 s}+C_4e^{\mu_2 s} \tag{B5}$$

Here, $R_2^n(x) = -\frac{v_r^2}{v_l^2} F_2^{n''}(\frac{2cl_0 - v_r x}{v_l}) + \frac{\eta v_r - P}{m v_l^2} F_2^{n'}(\frac{2cl_0 - v_r x}{v_l}) - \frac{k}{m v_l^2} F_2^n(\frac{2cl_0 - v_r x}{v_l})$,

$$\begin{cases} G_2^n(l_0 + v_l(t_a + (n-1)T)) = G_3^n(l_0 + v_l(t_a + (n-1)T)) \\ G_2^{n'}(l_0 + v_l(t_a + (n-1)T)) = G_3^{n'}(l_0 + v_l(t_a + (n-1)T)) \end{cases}, \begin{cases} C_3 = \frac{G_2^{n'}(l_0 + v_l(t_a + (n-1)T))}{e^{\mu_1(l_0 + v_l(t_a + (n-1)T))}(\mu_1 - \mu_2)} \\ \quad - \frac{\mu_2 G_2^n(l_0 + v_l(t_a + (n-1)T))}{e^{\mu_1(l_0 + v_l(t_a + (n-1)T))}(\mu_1 - \mu_2)} \\ C_4 = \frac{G_2^{n'}(l_0 + v_l(t_a + (n-1)T))}{e^{\mu_2(l_0 + v_l(t_a + (n-1)T))}(\mu_2 - \mu_1)} \\ \quad - \frac{\mu_1 G_2^n(l_0 + v_l(t_a + (n-1)T))}{e^{\mu_2(l_0 + v_l(t_a + (n-1)T))}(\mu_2 - \mu_1)} \end{cases}$$

Following results are for the case of $\beta$=1.

$$\mu = -\alpha = -\sqrt{\frac{k}{m v_l^2}} \tag{B6}$$

$$G_2^n(s) = e^{\mu s} \int_{l_0 + v_l(n-1)T}^{s} R_1^n(x) e^{-\mu x}(s-x)\mathrm{d}x + (C_3 + C_4 s)e^{\mu s} \tag{B7}$$

Here, $$\begin{cases} C_3 = \frac{(1 + \mu(l_0 + v_l(n-1)T)) G_1^n(l_0 + v_l(n-1)T)}{e^{\mu(l_0 + v_l(n-1)T)}} \\ \qquad - \frac{(l_0 + v_l(n-1)T) G_1^{n'}(l_0 + v_l(n-1)T)}{e^{\mu(l_0 + v_l(n-1)T)}} \\ C_4 = \frac{G_1^{n'}(l_0 + v_l(n-1)T) - \mu G_1^n(l_0 + v_l(n-1)T)}{e^{\mu(l_0 + v_l(n-1)T)}} \end{cases}$$

$$G_3^n(s) = \int_{l_0 + v_l(t_a + (n-1)T)}^{s} R_2^n(x) e^{\mu(s-x)}(s-x)\mathrm{d}x + (C_3 + C_4 s)e^{\mu s} \tag{B8}$$

Here, $$\begin{cases} C_3 = \frac{(1 + \mu(l_0 + v_l(t_a + (n-1)T))) G_1^n(l_0 + v_l(t_a + (n-1)T))}{e^{\mu(l_0 + v_l(t_a + (n-1)T))}} \\ \qquad - \frac{(l_0 + v_l(t_a + (n-1)T)) G_1^{n'}(l_0 + v_l(t_a + (n-1)T))}{e^{\mu(l_0 + v_l(t_a + (n-1)T))}} \\ C_4 = \frac{G_1^{n'}(l_0 + v_l(t_a + (n-1)T)) - \mu G_1^n(l_0 + v_l(t_a + (n-1)T))}{e^{\mu(l_0 + v_l(t_a + (n-1)T))}} \end{cases}$$